

The influence of zones outside of a cap on the radial component of the gravitational tensor as measured by a spaceborne gradiometer

Huseyin Baki Iz and Joseph Chan

ST Systems Corporation, Lanham, MD 20706, USA

Received January 23, 1990; Accepted October 17, 1990

Summary. A quick method to assess the influence of mean gravity anomalies - outside of a cap on the surface of the Earth - on the radial component of a spaceborne gradiometer is developed and evaluated for different mission parameters. A series expression as well as a recursive form to assess this effect is also derived. Numerical results indicate that the size of the region (cap size) is a more important factor in affecting the truncation errors than the altitude of the satellite. The availability of a high degree and order reference gravity field information reduces the regional truncation effect considerably (one order of magnitude for a spherical versus 18x18 degree and order harmonic reference field for a cap size of radius larger than 20°).

Introduction

Error analysis studies of satellite gradiometry can be exercised with respect to regional gravity field mapping and global gravity field mapping. Global approaches are usually based on the recovery of harmonic coefficients from the global measurements of a spaceborne gradiometer (e.g. Jekeli and Rapp 1980, Rapp 1988, Colombo 1989). These approaches are limited in the spectral information due to the use of a finite number of harmonic coefficients. The error due to the truncation can be evaluated using the well known harmonic representations (Jekeli and Rapp 1980). In regional or local gravity field mapping, mean local gravity anomalies are estimated from the gradiometer measurements within a cap on the surface of the Earth (Kahn et al. 1988). In this approach, the spectral information is limited by the size of the cap under consideration due to the omission of the gravity anomaly information outside the cap. The error due to the truncation must therefore be known in order to determine the effective cap size to be used in the recovery of local gravity anomalies from spaceborn gradiometer measurements.

In this study a quick method to assess the influence of

zones outside a cap on the radial component of the gravitational tensor as measured by a spaceborne gradiometer is developed and evaluated for different mission variables.

Mathematical model

An orbiting gravity gradiometer measures the second spatial derivative of the potential; the gravitational tensor Γ . Due to the conservative and symmetric nature of the Earth's gravity field only five tensor elements of nine are independent. We will consider the radial component Γ_{rr} of the gravity field tensor Γ , because it is the dominant component as compared to the others. From the classical relationship between the gravity potential $W(p)$ at a point p located outside the Earth and the normal potential $U(p)$ and the disturbing potential $T(p)$

$$W(p) = U(p) + T(p) \quad (1)$$

the second derivative of the gravity tensor is given by,

$$\Gamma_{rr}(p) = U_{rr} + T_{rr}(p) \quad (2)$$

Quasi-observations of T_{rr} can be obtained from the above expression for a given position of the orbiting instrument, the observed $\Gamma_{rr}(p)$, and an adopted normal potential. These quasi-observations can be related to the point gravity anomalies on the surface of the Earth using the following expression

$$T_{rr} = \frac{R}{4\pi} \int \int_{\sigma} \Delta g S_{rr}(r, \psi) d\sigma \quad (3)$$

where

$$S_{rr} = \frac{h^3}{R^2} \left[(1 - \cos\psi) \left(\frac{3 - 3h^2}{D^5} + \frac{4}{D^3} \right) - \frac{1 - h^2}{D^3} + \frac{10}{D} - 18D + 2 - 3h\cos\psi \left(15 + 6 \log \frac{1 - h\cos\psi + D}{2} \right) \right] \quad (4)$$

and

$$h := \frac{R}{r}, \quad D := \sqrt{1 + h^2 - 2h \cos\psi} \quad (5)$$

In these expressions, R is the mean radius of the Earth, r is the distance from the satellite to the center of mass of the Earth, T_{rr} is the second derivative of the disturbing potential with respect to the radial component, Δg is the point gravity anomaly on the surface of the Earth, S_{rr} is the second derivative of the Stokes function in the radial direction, and ψ is the spherical distance between the attracted point p and the surface element $d\sigma$. For a given point $p(r, \theta, \lambda)$, the above equations can also be written in terms of the spherical polar coordinates, α, ψ . Note that now ψ is made to coincide with the previously defined spherical distance. Accordingly, the surface element is defined as

$$d\sigma = \sin\psi \, d\psi \, d\alpha \quad (6)$$

Hence (3) can be expressed as

$$T_{rr} = \frac{R}{4\pi} \int_{\alpha=0}^{2\pi} \int_{\psi=0}^{\pi} \Delta g(\alpha, \psi) S_{rr}(r, \psi) \sin\psi \, d\psi \, d\alpha \quad (7)$$

The above equation can be *approximated* to a summation and the gravity anomalies can be treated as unknown parameters to be solved from the computed *quasi-observations*. The evaluation of the resulting observation equations however, would require the inclusion of a large number of observations (as well as a large number of unknowns) because the integration limits extend over the whole Earth. On the other hand, due to the rapid decay of the influence of distant anomalies on the measurements, observations may not contain *significant* gravity information beyond a certain area of radius ψ_T depending on the sensitivity (precision) of the instrument. In this case the mathematical model of observation equations (7) can be parametrized using only the gravity anomalies within a cap of certain size. Assessing the average effect of the gravity anomaly information on the *quasi-observations* outside an area is useful in deciding the cap size. A quick method is developed for this purpose.

Truncation Effect

For an arbitrary point $p(r, \theta, \lambda)$, (7) can be expressed as

$$T_{rr} = \frac{R}{4\pi} \int_{\alpha=0}^{2\pi} \int_{\psi=0}^{\psi_T} \Delta g S_{rr}(r, \psi) \sin\psi \, d\psi \, d\alpha + \frac{R}{4\pi} \int_{\alpha=0}^{2\pi} \int_{\psi=\psi_T}^{2\pi} \Delta g S_{rr}(r, \psi) \sin\psi \, d\psi \, d\alpha \quad (8)$$

If $\psi_T = \text{constant}$, denotes the radius of a cap which covers the region under consideration, then the second term in (8) is the effect of the point anomalies outside this region on the gradiometer measurements, i.e.

$$\delta T_{rr} := \frac{R}{4\pi} \int_{\alpha=0}^{2\pi} \int_{\psi=\psi_T}^{\pi} \Delta g S_{rr}(r, \psi) \sin\psi \, d\psi \, d\alpha \quad (9)$$

We now introduce a discontinuous function $\bar{S}_{rr}(r, \psi)$

$$\bar{S}_{rr}(r, \psi) = \begin{cases} 0 & \text{if } 0 \leq \psi \leq \psi_T \\ S_{rr}(r, \psi) & \text{if } \psi_T \leq \psi \leq \pi \end{cases} \quad (10)$$

then

$$\delta T_{rr} = \frac{R}{4\pi} \int_{\alpha=0}^{2\pi} \int_{\psi=0}^{\pi} \Delta g \bar{S}_{rr}(r, \psi) \sin\psi \, d\psi \, d\alpha \quad (11)$$

Let us now express $\bar{S}_{rr}(r, \psi)$ in terms of zonal harmonics

$$\bar{S}_{rr}(r, \psi) = \sum_{n=0}^{\infty} \frac{2n+1}{2} Q_n P_n(\cos\psi) \quad (12)$$

where the coefficients Q_n are expressed as

$$\frac{2n+1}{2} Q_n = \frac{2n+1}{4\pi} \int_{\alpha=0}^{2\pi} \int_{\psi=0}^{\pi} \bar{S}_{rr}(r, \psi) P_n(\cos\psi) \sin\psi \, d\psi \, d\alpha \quad (13)$$

The integration of (13) with respect to α gives

$$Q_n = \int_{\psi=\psi_T}^{\pi} S_{rr}(r, \psi) P_n(\cos\psi) \sin\psi \, d\psi \quad (14)$$

Let us substitute (12) into (11) and interchange the order of integration and summation. The following form is obtained

$$\delta T_{rr} = \frac{R}{4\pi} \sum_{n=0}^{\infty} \frac{2n+1}{2} Q_n \int_{\alpha=0}^{2\pi} \int_{\psi=0}^{\pi} \Delta g P_n(\cos\psi) \sin\psi d\psi d\alpha \quad (15)$$

Let us now express $\Delta g(\theta, \lambda)$ on the surface of the Earth into a series of spherical harmonics

$$\Delta g(\theta, \lambda) = \sum_{n=2}^{\infty} \Delta g_n(\theta, \lambda) \quad (16)$$

The integral in (15) is equal to $4\pi \Delta g_n / (2n+1)$, (Heiskanen and Moritz 1967). Considering (16), (15) can be written as

$$\delta T_{rr} = \frac{R}{2} \sum_{n=2}^{\infty} Q_n \Delta g_n(\theta, \lambda) \quad (17)$$

at $p(r, \theta, \lambda)$. In this expression, Δg_n is the n^{th} degree harmonic of Δg and (θ, λ) are its spherical coordinates. This equation represents the error in T_{rr} at a measurement point $p(r, \theta, \lambda)$ due to the omission of gravity anomalies outside of a cap of radius, ψ_r , centered at the footprint of p on the surface of the Earth. If we are interested in the effect of mean gravity anomalies ($\Delta \bar{g}$); from (17), we can express these mean effects as

$$\delta \bar{T}_{rr} = \frac{R}{2} \sum_{n=2}^{\infty} Q_n \Delta \bar{g}_n(\theta, \lambda) \quad (18)$$

Adopting the mean anomaly definition given by Jekeli and Rapp (1980)

$$\Delta \bar{g}(\theta, \lambda) = \frac{1}{2\pi(1-\cos\psi_0)} \iint_{\sigma} \Delta g d\sigma \quad (19)$$

where ψ_0 is the radius of a cap σ_c of area equal to the mean anomaly block, then

$$\Delta \bar{g}_n(\theta, \lambda) = \gamma \sum_{n=2}^{\infty} (n-1) \sum_{m=-n}^n \beta_n \bar{A}_{nm} \bar{Y}_{nm}(\theta, \lambda) \quad (20)$$

(ibid), and γ is the normal gravity. The n^{th} component of $\Delta \bar{g}$, from (20), is given by

$$\Delta \bar{g}_n(\theta, \lambda) = \gamma \sum_{m=-n}^n (n-1) \beta_n \bar{A}_{nm} \bar{Y}_{nm}(\theta, \lambda) \quad (21)$$

where the smoothing coefficients β_n are recursively given by (Sjoberg 1980)

$$\beta_n = \frac{2n-1}{n+1} \cos\psi_0 \beta_{n-1} - \frac{n-2}{n+1} \beta_{n-2} \quad (22)$$

$$\beta_0 = 1, \quad \beta_1 = \frac{1+\cos\psi_0}{2} \quad (23)$$

Substituting (21) into (18) and averaging (integrating) over the whole Earth leads to the mean squared effect on the gradiometer measurements of the mean gravity anomalies outside the region under consideration

$$\delta \bar{T}_{rr} = \frac{R}{2} \sum_{n=2}^{\infty} Q_n \sum_{m=-n}^n \gamma (n-1) \beta_n \bar{A}_{nm} \bar{Y}_{nm}(\theta, \lambda) \quad (24)$$

$$m(\delta \bar{T}_{rr})^2 = \frac{R^2}{4} \sum_{n=2}^{\infty} Q_n^2 \beta_n^2 C_n \quad (25)$$

In this expression, the gravity anomaly degree variances, C_n , are related to the spherical harmonics through the following expression

$$\sum_{m=-n}^n A_{nm}^2 = \frac{C_n}{\gamma^2 (n-1)^2} \quad (26)$$

Now, if a model for the gravity anomaly variances is postulated then the root mean squared (rms) influence of the remote zones on gradiometer measurements can be calculated using (25) and numerically integrating (14). The accumulation of the computational round-off errors inherent in all numerical quadrature techniques and the instabilities of the integration at higher degrees however, put a limitation on the accuracy of the results. A series representation for (14) can be used as an alternative to numerical quadratures.

Consider now the following representation for the Stokes function (Hotine 1969)

$$S(r, \psi) = \sum_{n=2}^{\infty} \frac{2n+1}{n-1} h^{n+1} P_n(\cos\psi) \quad (27)$$

where $h:=R/r$. The second partial derivative of (24) with respect to r gives

$$S_{rr}(r, \psi) = \sum_{n=2}^{\infty} \frac{(2n+1)(n+1)(n+2)}{(n-1)} h^{n+1} \left(\frac{1}{r^2}\right) P_n(\cos\psi) \quad (28)$$

The following expressions can easily be obtained from the integral properties of Legendre functions (Hobson 1965, Paul 1973)

$$R_{n,k}(t) := \int_{-1}^t P_n(t) P_k(t) dt = \quad (29)$$

$$\frac{\frac{n(n+1)}{2n+1} P_k(t) [P_{n+1}(t) - P_{n-1}(t)] - \frac{k(k+1)}{2k+1} P_n(t) [P_{k+1}(t) - P_{k-1}(t)]}{(n-k)(n+k+1)}$$

and

$$R_{n,n}(t) := \int_{-1}^t P_n(t) P_n(t) dt = \frac{(n+1)(2n-1)}{n(2n+1)} R_{n+1,n-1}(t) \quad (30)$$

$$- \frac{n-1}{n} R_{n,n-2}(t) + \frac{2n-1}{2n+1} R_{n-1,n-1}(t)$$

where $t := \cos\psi$. Now, substituting (29) and (30) into (14) and considering $dt = -\sin\psi d\psi$

$$Q_n = \frac{(2n+1)(n+1)(n+2)}{(n-1)} h^{n+1} \left(\frac{1}{r^2}\right) R_{n,n}(t) \quad (31)$$

$$+ \sum_{\substack{k=2 \\ k \neq n}}^{\infty} \frac{(2k+1)(k+1)(k+2)}{k-1} h^{k+1} \left(\frac{1}{r^2}\right) R_{k,n}(t)$$

is obtained. This series expression can be evaluated using (29), (30) and the recursive expression for the Legendre polynomials which are given by

$$P_n(t) = \frac{2n-1}{n} t P_{n-1}(t) - \frac{n-1}{n} P_{n-2}(t) \quad (32)$$

The initial values for the above expressions are

$$P_0(t) = 1, \quad P_1(t) = t, \quad (33)$$

$$R_{0,0} = t + 1, \quad R_{1,1} = (t^3 + 1)/3$$

Although (31) does not have the problems of instability in the evaluation of Q_n by the numerical quadrature, it involves infinite series which are not practical for problems which require the computation of Q_n for large n and k . This difficulty can be avoided if (31) is expressed recursively as shown in the following derivations.

Consider now the following partial fraction expressions for certain coefficients which are needed in the subsequent derivations. These expressions were obtained from software designed for symbolic mathematical operations. Although their derivations are somewhat cumbersome if performed by hand, they can be easily checked through simple algebraic manipulations). They are

$$\frac{(k+1)(k+2)^2(k+3)}{(n-k-1)(n+k+2)k} = -5 - k$$

$$- \frac{n^5 - n^4 - n^3 + n^2}{(n+2)(n-1)(2n+1)(k+n+2)} \quad (34)$$

$$- \frac{n^5 + 6n^4 + 13n^3 + 12n^2 + 4n}{(n+2)(n-1)(2n+1)(k-n+1)}$$

$$+ \frac{12}{(n+2)(n-1)k}$$

$$\frac{(2k+1)(k+1)(k+2)}{(k-1)(n-k)(n+k+1)} = -2$$

$$- \frac{2n^4 + 11n^3 + 21n^2 + 16n + 4}{(n+2)(n-1)(2n+1)(k-n)}$$

$$\frac{n^4 - 3n^3 + n}{(n+2)(n-1)(2n+1)(k+n+1)}$$

$$+ \frac{18}{(n+2)(n-1)(k-1)}$$

$$\frac{(k-1)k^2(k+1)}{(k-2)(n+k)(n-k+1)} = -3 - k$$

$$- \frac{n^5 + 6n^4 + 13n^3 + 12n^2 + 4n}{(n+2)(n-1)(2n+1)(k-n-1)} \quad (36)$$

$$- \frac{n^5 - n^4 - n^3 + n^2}{(n+2)(n-1)(2n+1)(k+n)}$$

$$+ \frac{12}{(n+2)(n-1)(k-2)}$$

Considering (32), (33), (34), (35) and (36), and re-writing the index of summation for $k = 2$ to ∞ , the following expression is obtained for (31)

$$Q_n = \frac{(2n+1)(n+1)(n+2)}{n-1} h^{n+1} \frac{1}{r^2} R_{n,n}(t)$$

$$+ \frac{1}{r^2} \{ \llbracket P_n(t) \sum_{\substack{k=1 \\ k \neq n-1}}^{\infty} - 5h^{k+2} P_k(t) - kh^{k+2} P_k(t) \rrbracket$$

$$- \frac{n^5 - n^4 - n^3 + n^2}{(n+2)(n-1)(2n+1)(k+n+2)} h^{k+2} P_k(t) \quad (37)$$

$$- \frac{n^5 + 6n^4 + 13n^3 + 12n^2 + 4n}{(n+2)(n-1)(2n+1)(k-n+1)} h^{k+2} P_k(t)$$

$$+ \frac{12}{(n+2)(n-1)k} h^{k+2} P_k(t) \rrbracket$$

$$\begin{aligned}
& + \left[\frac{n(n+1)}{2n+1} [P_{n+1}(t) - P_{n-1}(t)] \sum_{\substack{k=2 \\ k \neq n}}^{\infty} -2h^{k+1}P_k(t) \right. \\
& \quad + \frac{18}{(n+2)(n-1)(k-1)} h^{k+1}P_k(t) \\
& \quad - \frac{2n^4 + 11n^3 + 21n^2 + 16n + 4}{(n+2)(n-1)(2n+1)(k-n)} h^{k+1}P_k(t) \left. \right] \\
& \quad - \left[P_n(t) \sum_{\substack{k=3 \\ k \neq n}}^{\infty} -3h^kP_k(t) - kh^kP_k(t) \right. \\
& \quad + \frac{12}{(n+2)(n-1)(k-2)} h^kP_k(t) \\
& \quad - \frac{n^5 - n^4 - n^3 + n^2}{(n+2)(n-1)(2n+1)(k+n)} h^kP_k(t) \\
& \quad \left. - \frac{n^5 + 6n^4 + 13n^3 + 12n^2 + 4n}{(n+2)(n-1)(2n+1)(k-n-1)} h^kP_k(t) \right] \}
\end{aligned}$$

Let us now define,

$$U_n(t, h) := \sum_{\substack{k=0 \\ k \neq n-1}}^{\infty} \frac{h^{k-n+1}}{k-n+1} P_k(t); \quad h \leq 1 \quad (38)$$

$$V_n(t, h) := \sum_{k=0}^{\infty} \frac{h^{k+n+1}}{k+n+1} P_k(t); \quad h \leq 1 \quad (39)$$

Note that

$$\sqrt{1-2th+h^2} = \sum_{k=0}^{\infty} h^k P_k(t) \quad (40)$$

$$\begin{aligned}
\frac{\partial}{\partial h} \sqrt{1-2th+h^2} &= \sum_{k=0}^{\infty} k h^{k-1} P_k(t) \\
&= (t-h)(1-2th+h^2)^{-3/2}
\end{aligned} \quad (41)$$

and

$$\begin{aligned}
(1-2t\epsilon+h^2)^{1/2} &= 1-\epsilon t \\
&+ \sum_{k=1}^{\infty} \frac{P_{k-1}(t, h) - P_{k+1}(t, h)}{2k+1} \epsilon^{k+1}
\end{aligned} \quad (42)$$

In these expressions, U_n and V_n can be computed recursively. Considering the definition of V_n (39), and using (40) and (41), it can be shown that

$$\begin{aligned}
\int_{\epsilon}^h (1-2th+h^2)^{1/2} h^n dh &= V_n(t, h) - V_n(t, \epsilon) \\
0 < \epsilon < h \leq 1
\end{aligned} \quad (43)$$

Integrating (43) by parts and using (42) we obtain

$$\begin{aligned}
V_n(t, h) &= \frac{(2n-1)t V_{n-1}(t, h) - (n-1)V_{n-2}(t, h)}{n} \\
&+ \frac{(1-2th+h^2)^{1/2} h^{n-1}}{n}
\end{aligned} \quad (44)$$

The initial values for the above recursive form are given by

$$V_0(t, h) = \ln \left[\frac{(1-2th+h^2)^{1/2} + h - t}{1-t} \right] \quad (45)$$

$$V_1(t, h) = tV_0(t, h) + (1-2th+h^2)^{1/2} - 1 \quad (46)$$

Following the similar steps, the recursive form for $U_n(t, h)$ is given by

$$\begin{aligned}
U_n(t, h) &= \frac{(2n-3)tU_{n-1}(t, h) - (n-2)U_{n-2}(t, h)}{(n-1)} \\
&- \frac{(1-2th+h^2)^{1/2}}{h^{n-1}} + \frac{P_{n-3}(t) - P_{n-1}(t)}{2n-3}, \quad n \geq 3
\end{aligned} \quad (47)$$

The initial values for (47) are

$$U_0(t, h) = \ln \left[\frac{(1-2th+h^2)^{1/2} + h - t}{1-t} \right] \quad (48)$$

$$U_1(t, h) = \ln \left[\frac{2}{(1-th+h^2)^{1/2} - th + 1} \right] \quad (49)$$

$$U_2(t, h) = tU_1(t, h) - \frac{(1-2th+h^2)^{1/2}}{h-t} \quad (50)$$

Using (38) and (39), (37) can be expressed as

$$\begin{aligned}
Q_n &= \frac{(2n+1)(n+1)(n+2)h^{n+1}}{n-1} \frac{1}{r^2} R_{n,n}(t) \\
&+ \frac{1}{r^2} \{ P_n(t) [-5[h^2(1-2th+h^2)^{-1/2} \\
&\quad - h^2 - h^{n+1}P_{n-1}(t)] \\
&\quad - [(t-h)h^3(1-2th+h^2)^{-3/2} \\
&\quad - (n-1)h^{n+1}P_{n-1}(t)] \\
&\quad - \frac{n^5 - n^4 - n^3 + n^2}{(n+2)(n-1)(2n+1)} [V_{n+1}^*(t,h) \\
&\quad - V_{n-1}^*(t,h)] - \frac{n^5 + 6n^4 + 13n^3 + 12n^2 + 4n}{(n+2)(n-1)(2n+1)} \\
&\quad [U_n(t,h)^* - U_{n+2}(t,h)] \\
&\quad + \frac{12}{(n+2)(n-1)} [U_1^*(t,h) - U_3^*(t,h)] \quad (51) \\
&+ 3[(1-2th+h^2)^{-1/2} - (1+th) - \frac{1}{2}(3t^2-1)h^2 \\
&\quad - h^{n+1}P_{n+1}(t)] + h(t-h)(1-2th+h^2)^{-3/2} \\
&\quad - th - (3t^2-1)h^2 - (n+1)h^{n+1}P_{n+1}(t)] \\
&\quad + \frac{n(n+1)}{2n+1} [P_{n+1}(t) \\
&\quad - P_{n-1}(t)] [2[-h(1-2th+h^2)^{-1/2} \\
&\quad - h - th^2 - h^{n+1}P_n(t)] \\
&\quad + \frac{18}{(n+2)(n-1)} U_2^*(t,h) \\
&\quad - \frac{2n^4 + 11n^3 + 21n^2 + 16n + 4}{(n+2)(n-1)(2n+1)} U_{n+1}^*(t,h) \\
&\quad + \frac{2n^4 - 3n^3 + n}{(n+2)(n-1)(2n+1)} V_n^*(t,h)] \}
\end{aligned}$$

where

$$V_{n+1}^*(t,h) := h^{-n} [V_{n+1}(t,h) - \frac{h^{n+2}}{n+2} - \frac{h^{2n+1}}{2n+1} P_{n-1}(t)] \quad (52)$$

$$\begin{aligned}
V_n^*(t,h) &:= h^{-n} [V_n(t,h) - \frac{h^{n+1}}{n+1} \\
&\quad - \frac{th^{n+2}}{n+2} - \frac{h^{2n+1}}{2n+1} P_n(t)] \quad (53)
\end{aligned}$$

$$\begin{aligned}
V_{n-1}^*(t,h) &:= h^{-n} [V_{n-1}(t,h) - \frac{h^n}{n} - \frac{th^{n+1}}{n+1} \\
&\quad - \frac{3t^2-1}{2(n+2)} h^{n+2} - \frac{h^{2n+1}}{2n+1} P_{n+1}(t)] \quad (54)
\end{aligned}$$

$$\begin{aligned}
U_{n+2}^*(t,h) &:= h^{n+1} [U_{n+2}(t,h) + \frac{h^{-n-1}}{n+1} \\
&\quad + \frac{th^{-n}}{n} + \frac{3t^2-1}{2(n-1)} h^{-n+1}] \quad (55)
\end{aligned}$$

$$U_{n+1}^*(t,h) := h^{n+1} [U_{n+1}(t,h) + \frac{h^{-n}}{n} + \frac{th^{-n+1}}{n-1}] \quad (56)$$

$$U_n^*(t,h) := h^{n+1} [U_n(t,h) + \frac{h^{-n-1}}{n-1}] \quad (57)$$

$$U_3^*(t,h) := h^2 [U_3(t,h) + \frac{h^{-2}}{2} + th^{-1} - \frac{h^{-n-1}}{n-1} P_{n+1}(t)] \quad (58)$$

$$U_2^*(t,h) := h^2 [U_2(t,h) + h^{-1} - \frac{h^{-n-1}}{n-1} P_n(t)] \quad (59)$$

$$U_1^*(t,h) := h^2 [U_1(t,h) - \frac{h^{-n-1}}{n-1} P_{n-1}(t)] \quad (60)$$

Q_n , given in infinite series form in (51), can now be computed recursively using (44) through (50), and (52) through (60). Table 1 shows the Q_n values obtained from the series and the recursive representations.

Although remarkable agreement was obtained between the two approaches for $n < 500$, discrepancies occurred for larger values of n . A close examination of the terms in the recursive formulas revealed that successive computations of the recursive expressions for large n can lead to serious numerical round-off errors (catastrophic cancellation). When the recursive expressions were evaluated with increased computational precision both approaches gave similar results. The recursive expression, even if computed in quadruple precision arithmetic, is still 10 times faster than the series expression computations.

Table 1 Numerical Comparison of Recursive and Series Expressions

Satellite Altitude 160 Km, Cap Size 1/2 Degree			
Degree	Recursive Solution (Double Precision)	Recursive Solution (Quadruple Precision)	Series Solution (Double Precision)
2	0.13594062138686E+02	0.13594062138707E+02	0.13594062138699E+02
100	0.90729803717404E+01	0.90729803717309E+01	0.90729803717269E+01
200	-0.31283674790444E+01	-0.31283674795541E+01	-0.31283674795611E+01
300	-0.30058821255862E+01	-0.30058821343109E+01	-0.30058821343117E+01
400	-0.99182744723210E+00	-0.99182758651990E+00	-0.99182758651555E+00
500	0.46583398488629E+00	0.46583190174532E+00	0.46583190175127E+00
600	0.94836386824593E+00	0.94833397722825E+00	0.94833397723062E+00
700	0.66624823362690E+00	0.66583135941119E+00	0.66583135940874E+00
800	0.87460839426446E- 01	0.81766580746311E- 01	0.81766580741174E-01
900	-0.28836792953582E+00	-0.36492376940122E+00	-0.36492376940497E+00
1000	0.56147843535103E+00	-0.45497689145392E+00	-0.45497689145386E+00
1100	0.13125223783922E+02	-0.23479843448495E+00	-0.23479843448143E+00
1200	0.17422278484727E+03	0.81306633405281E- 01	0.81306633409100E-01
1300	0.22542835447690E+04	0.27451151695369E+00	0.27451151695550E+00
1400	0.29001701959543E+05	0.25026384119769E+00	0.25026384119711E+00
1500 ^(*)	0.37123841325998E+06	0.68147234631628E- 01	0.68147234638415E-01

Satellite Altitude 200 Km, Cap Size 1/2 Degree			
Degree	Recursive Solution (Double Precision)	Recursive Solution (Quadruple Precision)	Series Solution (Double Precision)
2	0.17073974447763E+02	0.17073974447783E+02	0.17073974447778E+02
100	0.48025231697029E+01	0.48025231698632E+01	0.48025231698613E+01
200	-0.24229417723611E+01	-0.24229417660693E+01	-0.24229417660730E+01
300	-0.17447651081046E+01	-0.17447648995959E+01	-0.17447648995961E+01
400	-0.50049918578789E+00	-0.50049305501221E+00	-0.50049305500964E+00
500	0.31551520148661E+00	0.31568403602404E+00	0.31568403602749E+00
600	0.55868831691742E+00	0.56314962556378E+00	0.56314962556509E+00
700	0.26538761056839E+00	0.37996660443200E+00	0.37996660443051E+00
800	-0.28469844907251E+01	0.35158408015770E- 01	0.35158408012751E-01
900	-0.71577651690233E+02	-0.22091408184249E+00	-0.22091408184465E+00
1000	-0.17449767654290E+04	-0.26656559022164E+00	-0.26656559022155E+00
1100	-0.42230079439086E+05	-0.13332575617955E+00	-0.13332575617718E+00
1200	-0.10136636995069E+07	0.52105021882331E- 01	0.52105021891247E-01
1300	-0.24161599547725E+08	0.16285276419758E+00	0.16285276435766E+00
1400	-0.57249027436007E+09	0.14579700804922E+00	0.14579701181766E+00
1500 ^(*)	-0.13495206885547E+11	0.37598385645152E- 01	0.37598474495235E-01

(*) CPU time for series expression (IBM 3081, double precision): 116.8 sec
CPU time for recursive expression (IBM 3081, double precision): 0.5 sec
CPU time for recursive expression (IBM 3081, quadruple precision): 12.1 sec

Numerical results

The truncation errors of the remote mean gravity anomalies are given in Figure 1. Satellite altitudes 160 km and 200 km were considered and truncation errors were computed for varying cap sizes. A spherical reference field was assumed in computing the quasi-observations, T_n , the second radial derivative of the disturbing potential. The covariance function model of Jekeli (1978) was adopted for computing the gravity anomaly degree variances, C_n , in equation (25). Figure 1 displays the truncation error differences of different block sizes with respect to the $1/2^\circ$ block size in order to emphasize the very small differences due to the change in

block size. Results indicate that the truncation error reduces, sharply for increasing cap sizes, and then slowly oscillates about a constant value for cap sizes up to 150° . Thereafter, they decrease sharply again to zero at 180° cap size. Truncation errors do not show any significant change for larger block sizes ($1^\circ \times 1^\circ$, $2^\circ \times 2^\circ$, $5^\circ \times 5^\circ$). The oscillating behavior of the truncation errors is due to the properties of the Stokes function and the minimum at about 115° cap size indicates error cancellation at certain cap sizes (locally optimal).

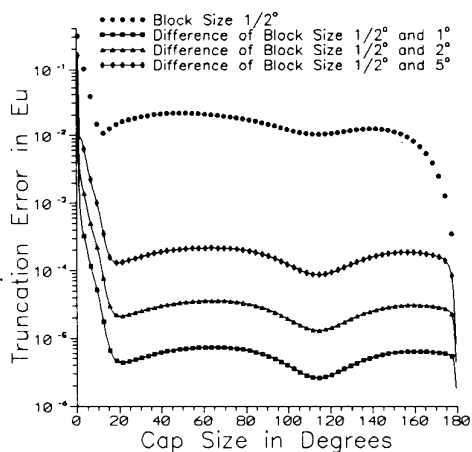


Fig 1. Altitude:160 Km, reference field:point mass. The differences of truncation errors of different block sizes are with respect to the $1/2^\circ$ block size truncation errors.

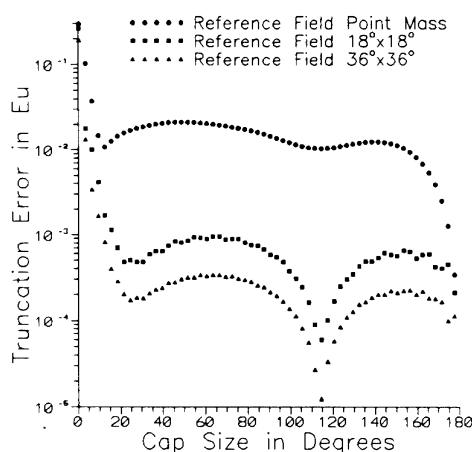


Fig 2. Variation of the truncation error as a function of cap size at 160 km satellite altitude. Block size $1/2^\circ$.

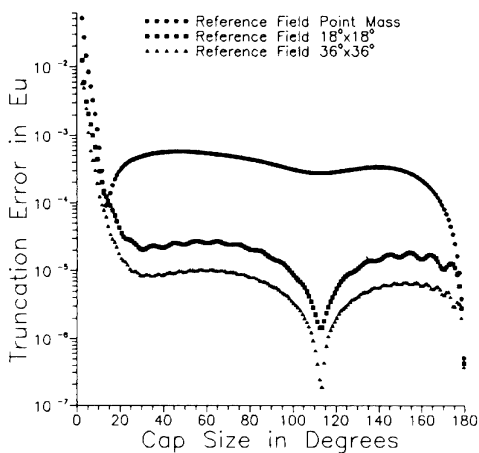


Fig 3. Truncation error differences between 160 km and 200 km for $1/2^\circ$ block size.

Table 2 Truncation error differences (in Eu) between 160 km vs 200 km for different block sizes with point mass reference field.

Cap Size	Block Size			
	$1/2^\circ$	1°	2°	5°
2.5	0.50879E-01	0.50684E-01	0.50038E-01	0.46874E-01
3.5	0.26665E-01	0.26546E-01	0.26185E-01	0.24703E-01
4.5	0.14527E-01	0.14468E-01	0.14289E-01	0.13567E-01
5.5	0.84718E-02	0.84408E-02	0.83448E-02	0.79507E-02
6.5	0.52077E-02	0.51898E-02	0.51334E-02	0.48965E-02
7.5	0.32923E-02	0.32809E-02	0.32445E-02	0.30886E-02
8.5	0.20706E-02	0.20626E-02	0.20368E-02	0.19238E-02
9.5	0.12339E-02	0.12277E-02	0.12074E-02	0.11173E-02
10.5	0.65494E-03	0.64993E-03	0.63345E-03	0.55987E-03
11.5	0.30121E-03	0.29749E-03	0.28521E-03	0.23094E-03
12.5	0.13665E-03	0.13419E-03	0.12612E-03	0.90893E-04
13.5	0.91569E-04	0.90053E-04	0.85059E-04	0.63438E-04
14.5	0.10432E-03	0.10338E-03	0.10028E-03	0.86771E-04
15.5	0.13966E-03	0.13905E-03	0.13703E-03	0.12804E-03
50.5	0.57862E-03	0.57842E-03	0.57765E-03	0.57268E-03
100.5	0.31367E-03	0.31357E-03	0.31319E-03	0.31066E-03
150.5	0.30889E-03	0.30872E-03	0.30807E-03	0.30388E-03

Table 3. Truncation error differences (in Eu) between 160 km and 200 km for different block sizes with $18^\circ \times 18^\circ$ reference field.

Cap Size	Block Size			
	$1/2^\circ$	1°	2°	5°
2.5	0.12440E-01	0.12050E-01	0.11007E-01	0.85618E-02
3.5	0.60095E-02	0.56435E-02	0.46581E-02	0.25425E-02
4.5	0.31575E-02	0.29695E-02	0.24314E-02	0.71430E-03
5.5	0.20729E-02	0.19812E-02	0.17098E-02	0.73085E-03
6.5	0.14399E-02	0.13910E-02	0.12425E-02	0.66971E-03
7.5	0.99236E-03	0.96361E-03	0.87494E-03	0.52144E-03
8.5	0.67012E-03	0.65179E-03	0.59500E-03	0.36900E-03
9.5	0.44453E-03	0.43198E-03	0.39327E-03	0.24362E-03
10.5	0.29406E-03	0.28491E-03	0.25682E-03	0.15223E-03
11.5	0.20097E-03	0.19397E-03	0.17248E-03	0.93575E-04
12.5	0.14890E-03	0.14349E-03	0.12677E-03	0.63895E-04
13.5	0.12136E-03	0.11723E-03	0.10433E-03	0.54205E-04
14.5	0.10457E-03	0.10142E-03	0.91431E-04	0.51381E-04
15.5	0.90878E-04	0.88406E-04	0.80510E-04	0.48044E-04
50.5	0.24503E-04	0.23831E-04	0.21649E-04	0.12549E-04
100.5	0.86658E-05	0.84341E-05	0.76787E-05	0.45024E-05
150.5	0.16128E-04	0.15677E-04	0.14216E-04	0.81707E-05

Table 4. Truncation error differences (in Eu) between 160 km and 200 km for different block sizes with 36°x36° reference field.

Cap Size	Block Size			
	1/2°	1°	2°	5°
2.5	0.58375E-02	0.51628E-02	0.31950E-02	0.60783E-03
3.5	0.49782E-02	0.45437E-02	0.33476E-02	0.44244E-03
4.5	0.25094E-02	0.23048E-02	0.17546E-02	0.22809E-03
5.5	0.11077E-02	0.99761E-03	0.71724E-03	0.13138E-03
6.5	0.59157E-03	0.52537E-03	0.35224E-03	0.55478E-04
7.5	0.42908E-03	0.39011E-03	0.28350E-03	0.31794E-04
8.5	0.30566E-03	0.28116E-03	0.21278E-03	0.30660E-04
9.5	0.19546E-03	0.17895E-03	0.13375E-03	0.22448E-04
10.5	0.12389E-03	0.11191E-03	0.79635E-04	0.12215E-04
11.5	0.93213E-04	0.84429E-04	0.60371E-04	0.70506E-05
12.5	0.78036E-04	0.71574E-04	0.53442E-04	0.72751E-05
13.5	0.61791E-04	0.56876E-04	0.43029E-04	0.68052E-05
14.5	0.45377E-04	0.41490E-04	0.30728E-04	0.49016E-05
15.5	0.34244E-04	0.31066E-04	0.22337E-04	0.29858E-05
50.5	0.96636E-05	0.88434E-05	0.65338E-05	0.90101E-06
100.5	0.33527E-05	0.30698E-05	0.22720E-05	0.31706E-06
150.5	0.64097E-05	0.58613E-05	0.43204E-05	0.60721E-06

Smaller truncation errors would be obtained if an accurate high degree and order gravity field is used for the reference field. When computing the truncation errors in the presence of a $n \times n$ degree and order reference field, the summation in equation (25) starts at $n+1$. Figure 2, shows the truncation effects in the presence of 18x18 and 36x36 reference fields. Once again, these errors reduce sharply for increasing cap sizes and start oscillating quite rapidly after cap size 25° with an amplitude less than 10^{-4} Eu around cap size 115°. Nevertheless, since no reference field is perfect, additional consideration should be given to the effect of their uncertainties in practice.

In Figure 3 the truncation errors between 160 km and 200 km for 1/2° block size was plotted for three different reference fields. Tables 2,3 and 4 show the effects of altitude on truncation errors, where the truncation error differences between 160 km and 200 km for different block sizes are tabulated for different reference fields. We observed significant reduction in the truncation errors as a result of increasing satellite altitude when considering small cap sizes ($<5^\circ$) only, and this effect diminishes very quickly as the cap sizes increase.

Conclusion

We have derived and demonstrated a quick method to assess the influence of remote mean gravity anomalies on a radial component measurement of a spaceborne gradiometer. Numerical results indicate that this influence is least affected by the altitude of the spacecraft but more by the size of the region (cap size) under consideration. The availability of a

high degree and order reference gravity field reduces the regional truncation effect considerably (one order of magnitude for a spherical versus 18x18 harmonic reference field for cap size radius larger than 20°). Overall, the effect of anomalies outside of a cap remain above 10^{-4} Eu which is a realizable superconducting gravity gradiometer accuracy in the future. Therefore the truncation effect is an important factor to be considered in modelling gradiometer measurements at this accuracy level. The effect of *very distant* zones is expected to remain constant within a region (but varying from region to region) leaving the regional gravity signature intact. Anomaly blocks surrounding the region will nevertheless introduce varying effects on the measurements which will affect the local gravity signature. Modelling for these effects will need further investigations.

References

- Colombo OL (1989) Advanced Techniques for High-Resolution Mapping of the Gravity Field, in Theory of Satellite Geodesy and Gravity Field Determination, F Sanso, R Rummel (Eds.), Springer-Verlag.
- Heiskanen WA, Moritz H (1967) Physical Geodesy, WH Freeman and Comp., San Francisco and London.
- Hobson EW (1965) The Theory of Spherical and Ellipsoidal Harmonics, Chelsea Publishing Corp., New York.
- Jekeli C (1978) An Investigation of the two models for the Degree Variances of Global Covariance Functions, Report No. 275, Dept. of Geodetic Science and Surveying, Columbus, Ohio.
- Jekeli C, Rapp R (1980) Accuracy of the Determination of Mean Anomalies and Mean Geoid Undulations from a Satellite Gravity field Mapping Mission, Report No. 307, OSU, Dept. of Geodetic Science and Surveying, Columbus, Ohio.
- Kahn W, Iz HB, Brown RD (1988) Estimation of Local Mean Gravity Anomaly Errors Using a Spaceborne Gravity Gradiometer, presented at the 1988 AGU Baltimore Meeting.
- Paul MK (1973) A Method of Evaluating the Truncation Error Coefficients for Geoidal Height, Bulletin Geodesique, Vol. 78, 1973.
- Rapp RH (1988) Signals and Accuracies to be Expected from a Satellite Gradiometer Mission, OSU, Dept. of Geodetic Science and Surveying, Columbus.
- Sjoberg L (1980) A Recurrence Relation for the β_n Function, Bulletin Geodesique, Vol. 54, No. 1, pp 69-72.